

A Close Examination of the Multipath Propagation Stochastic Model for Communications over Power Lines

José A. Cortés*, Alberto Pittolo†, Irene Povedano*, Francisco J. Cañete*, and Andrea M. Tonello*

Abstract—This paper focuses on the parameterization of the multipath propagation model (MPM) for indoor broadband power line communications (PLC), which up to now has been established in an heuristic way. The MPM model was originally proposed for outdoor channels in the band up to 20 MHz, but its number of parameters becomes extremely large when used to model indoor channel frequency responses (CFR), which are much more frequency-selective than outdoor ones, and the band is extended to 80 MHz. This work proposes a fitting procedure that addresses this problem. It allows determining the model parameters that yield the best fit to each channel of a large database of single-input single-output (SISO) experimental measurements acquired in typical home premises of different European countries. Then, the properties of the MPM parameters are analyzed. The study unveils the relation between the model parameters and the main characteristics of the actual CFR like the frequency selectivity and the average attenuation. It also estimates the probability density function (PDF) of each parameter and proposes a fitting distribution for each of them. Moreover, the relationship among the main parameters of the model is also explored. Provided results can be helpful for the development of MPM-based models for indoor broadband PLC.

Index Terms—Power line communications (PLC), channel model, multipath propagation model, channel frequency response, statistical characterization, probability density function.

I. INTRODUCTION

THE increasing demand of high-speed multimedia services led to reconsider the indoor power delivery network as a data transmission medium. The power line communication (PLC) technology is becoming an established solution since it exploits the existing wired infrastructure to convey high-speed data content, thus saving costs and deployment time. Furthermore, the latest standards and devices include advanced signal processing and enhanced transmission techniques, such as the exploitation of all the deployed network conductors and the bandwidth extension, that improve even further the achievable data rate, guaranteeing transmission rates in the order of gigabit per second at the physical layer [1]–[3].

*José A. Cortés, Irene Povedano and Francisco J. Cañete are with the Communications and Signal Processing Lab, Telecommunication Research Institute (TELMA), Universidad de Málaga, E.T.S.I. Telecomunicación, 29010 Málaga, Spain.

†Alberto Pittolo is with the University of Udine, Udine 33100, Italy.

*Andrea M. Tonello is with the Institute of Networked and Embedded Systems, Alpen-Adria-Universität Klagenfurt, Klagenfurt 9020, Austria.

This work has been partially supported by the Spanish Government under project PID2019-109842RBI00/AEI/10.13039/501100011033 and the University of Málaga under project PAR 15/2023.

This high performance level motivates a renewed interest in developing novel and updated PLC solutions, especially for home networking and smart grid applications [4]–[8].

In order to support the growth of PLC technology, it is fundamental to provide effective channel models, which are able to numerically emulate the properties of actual PLC networks avoiding on field tests. Two basic approaches can be tackled in defining a model, i.e., bottom-up and top-down, and both of them can follow a deterministic or a statistical strategy [9]–[12]. A deterministic strategy typically considers a specific network configuration, while a statistical strategy attempts to introduce some variability by means of statistical distributions. Concerning the possible approaches, the bottom-up method has a strong physical connection and describes the phenomena involved in the signal propagation by exploiting the transmission line theory. Typically, it provides a faithful channel representation, although it turns out to be a computationally onerous procedure. Some examples concerning the single-input-single-output (SISO) channel modeling can be found in [13], [14], which propose a deterministic approach, and in [11], [15]–[18], which follow a statistical approach. Recently, the models discussed in [19] and [20] extends the SISO bottom-up strategy to the multiple-input multiple-output (MIMO) case.

Conversely, the top-down approach is an empirical method that fits an analytic function to a measurements database. This strategy facilitates the statistical extension by adopting a certain distribution for the parameters that describe the theoretical function. One of the first and more common SISO models is the multipath propagation model (MPM) proposed in [9] and was later statistically extended in [21]. Extensions of the SISO formulation to the MIMO are presented in [22] and [23].

The PLC channel response also exhibits a short-term variation synchronous with the mains voltage, which allows modelling it as a linear periodically time-varying (LPTV) system [24]. However, since the time variation is quite small compared to the duration of the impulse response, i.e., the channel response is underspread, the slow variation approximation can be made and the channel response can be modeled as a series of time-invariant responses that repeat with the period of the mains signal. Hence, the MPM model can be applied to each of these time-invariant responses.

A. Contribution

The top-down MPM model formulated in [9] has been widely used in the PLC scenario [10], [25]–[28]. However, it was proposed for outdoor PLC channels in the band up to 20 MHz. Its statistical extension to indoor channels made in [29] and [21] was based on heuristic approaches and no rigorous measurement-based analysis of this model for indoor scenarios in the band up to 80 MHz has been found in the literature.

In this context, we make three main contributions:

- We propose a method to determine the parameters of the MPM model for indoor broadband PLC channels in the band up to 80 MHz. It addresses the problem of the extremely large number of parameters that results when the MPM model in [9] is extended to indoor scenarios and that are a consequence of the much more frequency selective behavior of indoor channel frequency responses (CFRs) and of the bandwidth extension to 80 MHz. Since interference with commercial frequency modulation (FM) broadcasting is important above 87 MHz in many regions.
- The proposed method has been used to perform a channel-by-channel fitting, determining the set of MPM parameters that yields the best approximation to each of the channels of a large database consisting of 426 CFRs measured in indoor scenarios of different European countries.
- We give an in-depth analysis of the resulting MPM parameters, showing their relation to the main channel characteristics like the frequency selectivity and the average attenuation, assessing their statistical behavior and the relation between them. Unlike the a posteriori parameters inference discussed in previous works, this study unveils the intrinsic properties of the MPM parameter and can be helpful for the development of novel MPM models or the refinement of existent ones.

B. Organization

The paper is organized as follows. First, the MPM is briefly recalled in Section II. Second, the assumptions and the method proposed to determine the MPM parameters that give the best fit to each measured channel is detailed and justified in Section III. The properties of the computed parameters, such as their relation to the channel characteristics, statistical behavior and relation between them are discussed in Section IV. Finally, conclusions follow in Section V.

II. BACKGROUND: THE MULTIPATH PROPAGATION MODEL

The MPM follows a top-down approach and describes the multipath propagation of the power signal into the PLC medium that is due to the line discontinuities, such as branches, or unmatched loads. The analytic formulation of the CFR can be expressed as [9]

$$H(f) = A \sum_{i=0}^{N-1} g_i e^{-(a_0+a_1 f^K) d_i} e^{-j2\pi f d_i/v}, \quad (1)$$

where a_0 and a_1 are the attenuation coefficients, g_i and d_i are the path gain and the path length of the i -th path¹, respectively. The coefficient g_i can be interpreted as the product of transmission and reflection coefficients by restricting $|g_i| \leq 1$ and by introducing the normalization coefficient $A > 0$, which allows adjusting the attenuation of the resulting CFR [9]. The term N denotes the number of paths and K is the exponent of the attenuation factor related to the cable features. This work uses $N = 2554$ (its rationale will be justified in Section III.III-B), which is much larger than the values used in outdoor channels. Typical values of K range between 0.5 and 1 [9], hence $K = 1$ is assumed for the rest of this paper. The parameter $v = c\epsilon_r$ is the propagation speed of light in the cables, where c is the speed of light in the vacuum and ϵ_r is the relative dielectric constant of the insulator which envelops the conductors, which has been set to $\epsilon_r = 1.5$ in order to take into account the non-uniformity of the dielectric [9].

III. DETERMINATION OF THE MPM PARAMETERS

In order to provide a statistical characterization of the parameters that describe the MPM formulation in (1), the first step is to compute the MPM parameters that give the best fitting of this analytic expression to each of the channels of the measurement database. The latter consists of 426 indoor CFRs measured in different European countries using a vector network analyzer. CFRs have $M = 1262$ frequency samples given by $f_m = f_0 + m\Delta f$, with $f_0 = 1.0$ MHz, $0 \leq m \leq M - 1$ and $\Delta f = 62.5978$ kHz. Part of this collection was previously used in [23] and [12], and the results are consistent with the ones obtained from other extensive measurements in Italy that were characterized in [30].

Since the model is described by many parameters, the following assumptions must be adopted in order to simplify the fitting strategy. First, the attenuation coefficients a_0 and a_1 are estimated through the robust regression fit of each channel measurement. This linear attenuation profile can be assumed to be essentially determined by the longest path of the MPM. Hence, we consider the model in (1) with a single path of the largest length, L (its value will be given in Section III.III-B). Since A is a normalization factor used to force $|g_i| \leq 1$, when a single path is considered it happens that $|A \cdot g_i| = 1$. Accordingly, the robust regression fit of the longest path in (1) can be expressed as

$$10 \log_{10} |H(f)|^2 = -2(a_0 + a_1 f)L \cdot 10 \log_{10} e = \alpha_0 + \alpha_1 f, \quad (2)$$

where α_0 and α_1 are the coefficients of the robust regression fit. Thus, the attenuation coefficients are computed as

$$a_0 = -\frac{\alpha_0}{20L \log_{10} e}, \quad a_1 = -\frac{\alpha_1}{20L \log_{10} e}. \quad (3)$$

Second, the path lengths are discretized yielding uniformly spaced distances,

$$d_i = i \frac{L}{N} \quad \text{with } i = 0, \dots, N - 1. \quad (4)$$

¹For the sake of notation simplicity in the subsequent fitting process, paths have been indexed as $0 \leq i \leq N - 1$, instead of $1 \leq i \leq N$ as done in [9].

This is a viable assumption since indoor PLC networks typically exhibit a complex topology with a great number of branches. This results into approximately uniformly distributed distances (spaced 1.25 m for the values of L and N considered in this work) traveled by the signal and its reflections from the transmitter side towards the receiver outlet.

Afterwards, the path gains, g_i that give the best fitting to each each measured channel have to be determined. This could be done by means of a least squares (LS) estimation that minimizes the root mean square error (RMSE) w.r.t. the measured channel in the set of M measured frequencies f_m ,

$$\text{RMSE} = \sqrt{\frac{1}{M} \sum_{m=0}^{M-1} |H(f_m) - \hat{H}(f_m)|^2}, \quad (5)$$

where $H(f_m)$ and $\hat{H}(f_m)$ represent the measured and fitted CFR at frequency f_m , respectively.

However, the RMSE is dominated by the error in the largest values of the CFR. Since the amplitude response of PLC is strongly frequency-selective, this causes the fitting to be very accurate at lowly attenuated values to the detriment of the fitting of the highly attenuated values. To avoid this end and achieve a balanced error distribution along the entire amplitude range, we determine the path gains that minimize the normalized root mean square error (NRMSE) defined as

$$\text{NRMSE} = \sqrt{\frac{1}{M} \sum_{m=0}^{M-1} \frac{|H(f_m) - \hat{H}(f_m)|^2}{|H(f_m)|^2}}. \quad (6)$$

The g_i can be obtained by solving a weighted LS (WLS) problem formulated by expressing (1) in matrix form as follows,

$$\underbrace{\begin{bmatrix} H(f_0) \\ \vdots \\ H(f_{M-1}) \\ H^*(f_{M-1}) \\ \vdots \\ H^*(f_0) \end{bmatrix}}_{\mathbf{h}} = \underbrace{\begin{bmatrix} P_{0,0} & \cdots & P_{0,N-1} \\ \vdots & & \vdots \\ P_{M-1,0} & \cdots & P_{M-1,N-1} \\ P_{M-1,0}^* & \cdots & P_{M-1,N-1}^* \\ \vdots & & \vdots \\ P_{0,0}^* & \cdots & P_{0,N-1}^* \end{bmatrix}}_{\mathbf{P}} \underbrace{\begin{bmatrix} g_0 \\ \vdots \\ g_{N-1} \end{bmatrix}}_{\mathbf{g}} \quad (7)$$

where $P_{m,i} = \exp(-(a_0 + a_1 f_m) d_i) \cdot \exp(-j2\pi f_m d_i / v)$ and the scaling factor A has been set to 1 by now.

By defining the weighting matrix

$$\mathbf{W} = \text{diag} \left\{ \frac{1}{|H(f_0)|^2}, \frac{1}{|H(f_1)|^2}, \dots, \frac{1}{|H(f_{M-1})|^2}, \frac{1}{|H(f_{M-1})|^2}, \dots, \frac{1}{|H(f_1)|^2}, \frac{1}{|H(f_0)|^2} \right\}, \quad (8)$$

the values of g_i can be obtained as

$$\mathbf{g} = (\mathbf{P}^H \mathbf{W} \mathbf{P})^{-1} \mathbf{P}^H \mathbf{W} \mathbf{h}. \quad (9)$$

A. Dominant Paths Selection Procedure

In order to fit each measured channel with a reduced set of parameters, paths with negligible contribution can be deleted, while keeping the most significant ones. To this

end, a decimation procedure that iteratively discards the path with the smallest contribution to approximate the measured CFR while keeping the NRMSE below a certain threshold is employed. The index of the path to be discarded at each iteration, designated as j , is determined as

$$j = \arg \min_i \left\{ \sum_m |g_i| e^{-(a_0 + a_1 f_m) d_i} \right\}. \quad (10)$$

The rationale for this criterion is that the actual contribution of a path to the overall CFR is essentially determined by the factor $|g_i| \cdot \exp(-(a_0 + a_1 f) d_i)$ in the MPM in (1).

The decimation procedure continues while the NRMSE (dB) remains lower than a given threshold, which has been set to -20 dB. This ensures that the channel computed with a reduced set of paths still represents a very good approximation to the corresponding measured channel. Since the columns of the matrix \mathbf{P} are not orthogonal, the path gains g_i have to be recomputed after a path is discarded. To this end, the problem in (7) is reformulated by removing the j -th column of the matrix \mathbf{P} and the new path gains are obtained. Table I summarizes the presented fitting and decimation procedure applied to each measured channel, where the expressions to obtain the values of L and N will be given in Section III.III-B.

When the decimation procedure ends, the path gains obtained for the considered measured channel are normalized by their maximum absolute value. This normalization factor provides the value for the parameter A . This way, the g_i values, which represent the product of transmission and reflection coefficients, are in the range $g_i \in [-1, 1]$, and the normalization coefficient $A \in (0, \infty)$.

The number of initial paths considered for the model at the pre-decimation point is $N = 2554$ (as justified in the next subsection). This gives average and standard deviation values of the NRMSE (computed over the set of measured channels) equal to $\overline{\text{NRMSE}} = -36.79$ dB and $\sigma_{\text{NRMSE}} = 7.99$ dB, respectively. After the application of the proposed decimation procedure, the number of paths is reduced to an average value (over the whole set of fitted channels) of 217.84, i.e., less than 10% of the initial value, and the corresponding average and standard deviation values of the NRMSE (dB) are $\overline{\text{NRMSE}} = -20.05$ dB and $\sigma_{\text{NRMSE}} = 0.0678$ dB, respectively. Hence, the proposed decimation process achieves a good trade-off between modeling complexity and accuracy.

For illustrative purposes, Fig.1 shows the amplitude and unwrapped phase of a measured CFR, $H(f)$, and its corresponding fitted response, $\hat{H}(f)$, obtained with $N = 183$ dominant paths determined using the proposed decimation process. As can be observed, the measured trace is almost veiled by the estimated one, which highlights the notable accuracy of the fitting process.

The procedure described up to now assumed an initial number of paths, N , and a maximum path length, L . These parameters cannot be chosen arbitrarily and their selection criteria are described in the following section.

B. Relation Among L , M , and N

The maximum length L , the maximum number of paths N , and the number of frequency samples M depend among each

Table I
ALGORITHM OF THE FITTING AND PATH SELECTION PROCEDURE APPLIED
TO EACH MEASURED CHANNEL

Algorithm: MPM fitting procedure

Input: \mathbf{h} (measured CFR) and $\text{NRMSE}_{\text{threshold}} = -20$ dB
Output: N (number of dominant paths), \mathbf{d} (path lengths), \mathbf{g} (path gains) and $\hat{\mathbf{h}}$ (fitted version of \mathbf{h})

- 1: Initialize L and N using (12) and (15), respectively
- 2: Initialize \mathbf{d} using (4)
- 3: Compute a_0 and a_1 using (3)
- 4: Compute \mathbf{g} using (9)
- 5: Compute $\hat{\mathbf{h}} = \mathbf{P}\mathbf{g}$
- 6: Compute the NRMSE using (6)
- 7: **while** NRMSE (dB) < NRMSE_{threshold} **do**
 - 8: Obtain j using (10)
 - 9: Calculate $\mathbf{P} = [\mathbf{P}(:, 0 : j - 1), \mathbf{P}(:, j + 1 : N - 1)]$
 - 10: Update \mathbf{g} using (9)
 - 11: Update $\hat{\mathbf{h}} = \mathbf{P}\mathbf{g}$
 - 12: Compute the NRMSE using (6)
 - 13: Update $N = N - 1$
- 14: **end while**
- 15: Compute $\mathbf{P} = [\mathbf{P}(:, 0 : j - 1), \mathbf{P}(:, j), \mathbf{P}(:, j + 1 : N - 1)]$
- 16: Update \mathbf{g} using (9)
- 17: Update $\hat{\mathbf{h}} = \mathbf{P}\mathbf{g}$

other and must satisfy certain constraints. Since only a discrete and finite number of frequencies is available, the expression in (1) given for the continuous frequency domain can be rewritten for the discrete domain as

$$H(f_m) = A \sum_{i=0}^{N-1} r_i e^{-j2\pi m \Delta f i \frac{L}{N\nu}}, \quad (11)$$

where $\Delta f = (f_{M-1} - f_0)/(M - 1)$ is the frequency resolution, while $\tau = L/(N\nu)$ is the time resolution. Note that the real part of the exponential term has been embedded within the corresponding path gain in a unique variable named r_i . The adopted notation does not affect the analysis since the real exponential part acts only as an attenuation term that increases with frequency. This way, equation (11) can be seen as a discrete time Fourier transform (DFT) with frequency index m and time index i . As known, the DFT assumes the time signal belonging to the domain of integer multiples of τ and periodic of $N\tau$. Such a domain is denoted with $\mathbb{Z}(\tau)/\mathbb{Z}(N\tau)$. Hence, in the frequency domain the signal is defined in $\mathbb{Z}(\Delta f)/\mathbb{Z}(N\Delta f)$, with $\Delta f = 1/(N\tau)$. Therefore, the relation between L and the frequency samples M is given by

$$\Delta f = \frac{f_{M-1} - f_0}{M - 1} = \frac{1}{N \frac{L}{N\nu}} = \frac{\nu}{L} \Rightarrow L = \frac{(M - 1)\nu}{f_{M-1} - f_0} \quad (12)$$

Since $f_{M-1} = 79.9358$ MHz and $f_0 = 1$ MHz, $M = 1262$ and the propagation speed is $\nu = 2 \cdot 10^8$ m/s, the maximum possible length that can be assumed is $L = 3195$ m. The limit of more than 3 kilometers turns out to be a maximum length that is long enough to describe any generic in-home

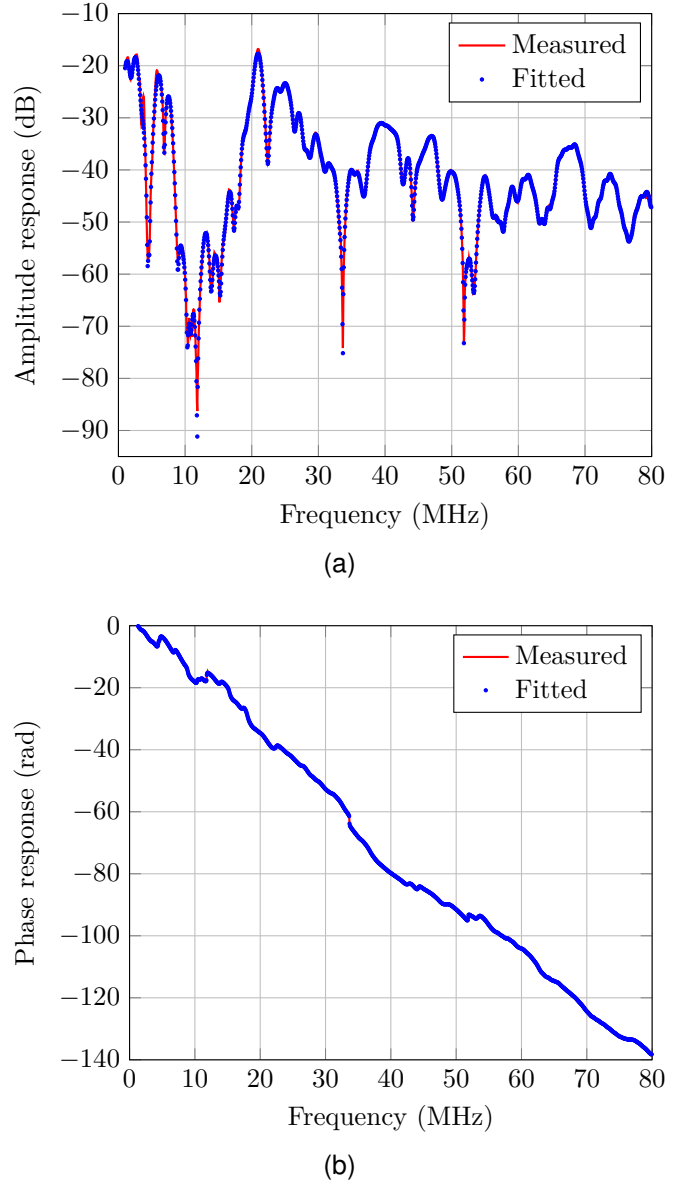


Figure 1. Amplitude (a) and unwrapped phase (b) response of a representative measured channel and its corresponding fitting determined with $N = 183$ dominant paths obtained with the proposed decimation procedure.

network topology. Moreover, always referring to the DFT representation of the CFR reported in (11), the DFT frequency period, i.e., $N\Delta f$, must be greater or equal than two times the maximum channel frequency, i.e., f_{M-1} , in order to avoid aliasing problems according to the sampling theorem. Thus, the relationship among N and L turns out to be

$$N\Delta f = \frac{1}{\tau} \geq 2f_{M-1} \Rightarrow N \geq \frac{2f_{M-1}L}{\nu}. \quad (13)$$

If the aforesaid values for f_{M-1} and ν are considered, the relation in (13) becomes $N \geq 0.8L$. A final relation among N and L can be noticed by rewriting the imaginary part of the exponential term in (1) as

$$e^{-j2\pi f d_i/\nu} = e^{-j2\pi k d_i/\lambda} \quad (14)$$

where $\lambda = v/\Delta f$ is the maximum possible wavelength, which is related to the frequency resolution Δf . The minimum observable wavelength is $\lambda_{min} = v/f_{M-1}$. Hence, to avoid numerical errors, the shortest (non-zero) path length $d_1 = \frac{L}{N}$ must be greater than $\lambda_{min}/2$, according to the sampling theorem. This provides the last relationship, expressed by

$$d_1 = \frac{L}{N} \geq \frac{\lambda_{min}}{2} \Rightarrow N \leq \frac{2f_{M-1}L}{v} \quad (15)$$

It can be noted that, given the above mentioned specifications, as well as the relations (13) and (15), the relationship among L and N must hold with equality, i.e., $N = 0.8L = 2554$ for the considered database.

IV. ANALYSIS OF THE MPM PARAMETERS

This section analyzes the statistical properties of the MPM parameters obtained according to the fitting procedure detailed in Section III for the overall set of measured channels. First, the relation of some model parameters to the main magnitudes used to characterize the channel response, such as the delay spread and the average channel gain. Then, the probability density function (PDF) of the MPM parameters is estimated and, finally, the statistical relation between the model parameters is studied.

A. Relation to the Channel Characteristics

The parameters a_0 and a_1 were obtained from the robust regression fit of the amplitude response of the measured channels, with a_1 being related to the slope of the attenuation profile and a_0 with the y-intercept. Hence, the latter parameter has to be somehow related to the average channel gain, defined as $G \text{ (dB)} = \frac{1}{M} \sum_{m=0}^{M-1} 20 \log_{10} |H(f_m)|$. This relation can be clearly observed in Fig. 2 (a), where the scatter plot of a_0 vs G (dB) is depicted, along with its robust fit regression line, whose expression is given in Table II. As expected, channels with larger average gains need lower values of a_0 to be synthesized.

The number of dominant paths needed to fit a given CFR is related to the frequency selectivity of the channel, e.g., a single path suffices to synthesize a *flat* channel. The frequency selectivity of a channel is usually quantified by means of the

coherence bandwidth or its inversely related magnitude, the delay spread (also referred to as multipath spread) [31]. In PLC these magnitudes are known to be related to the average channel gain [8]: channels with lower average channel gains tend to have larger delay spreads. Hence, these magnitudes are expected to be related to the number of dominant paths, N . Fig. 2 (b) illustrates this relation by showing the scatter plot of the number of dominant paths vs the average channel gain and the delay spread of the corresponding measured channel. Its robust regression plane, whose expression is given in Table II, is also depicted for reference. The goodness of this fit is confirmed by the NRMSE between the actual and predicted values of N , which is -22 dB.

The value of the normalization parameter A is also related to the average channel gain, as shown in Fig. 2 (c), which depicts the scatter plot of A vs G (dB) and its corresponding exponential fitting function. The parameters of the latter, which have been obtained by means of a LS fitting, are given in Table II. As observed, the lower the average channel gain, the lower the value of A needed to synthesize the channel.

B. Statistical Characterization

This subsection estimates the chief moments and the PDF of the MPM parameters, computed for the overall set of measured channels, that have been obtained using the fitting procedure presented in Section IV. For each empirical (estimated) PDF, the probability distribution that gives the best fit is given. To this end, the most common distribution functions are considered: beta, Birnbaum-Saunders, exponential, gamma, generalized extreme value (GEV), Gumbel, inverse Gaussian, logistic, log-logistic, log-normal, Nakagami, normal, Poisson, Rayleigh, Rician, t location-scale and Weibull. The parameters of each distribution that yield the best fit to the set of MPM parameters are obtained by means of the maximum likelihood (ML) estimation assuming independent samples [32]. Afterwards, the Anderson-Darling goodness-of-fit test is applied and the distribution yielding the highest p -value is selected. When the test gives the same p -value for all distributions or the null hypothesis is rejected for all of them, the one with the highest value of the likelihood function is selected. For

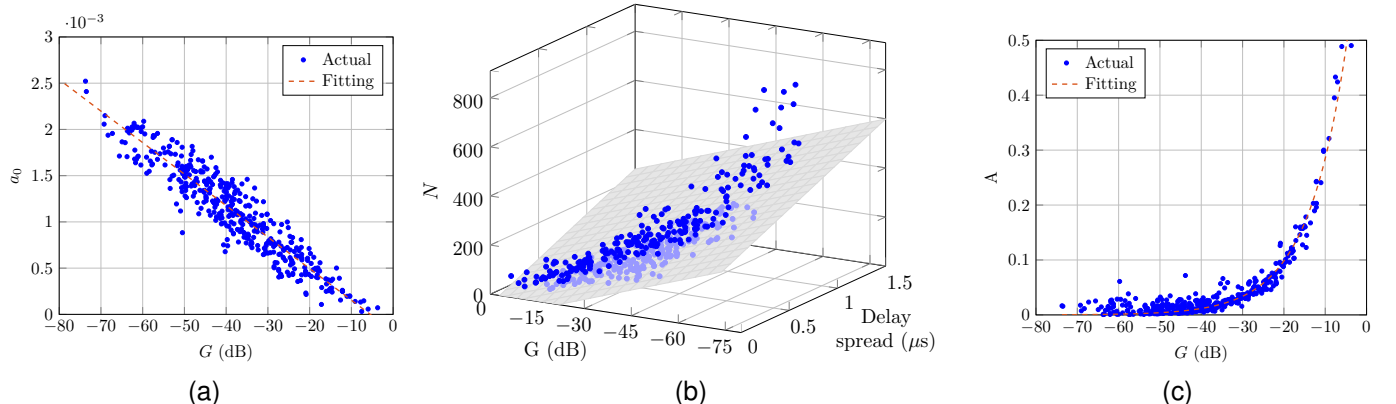


Figure 2. Scatter plot of (a) the value of a_0 vs the average channel gain of each measured channel, G (dB); (b) the number of dominant paths vs the average gain and the delay spread of the channels; (c) value of A vs the average channel gain of each measured channel.

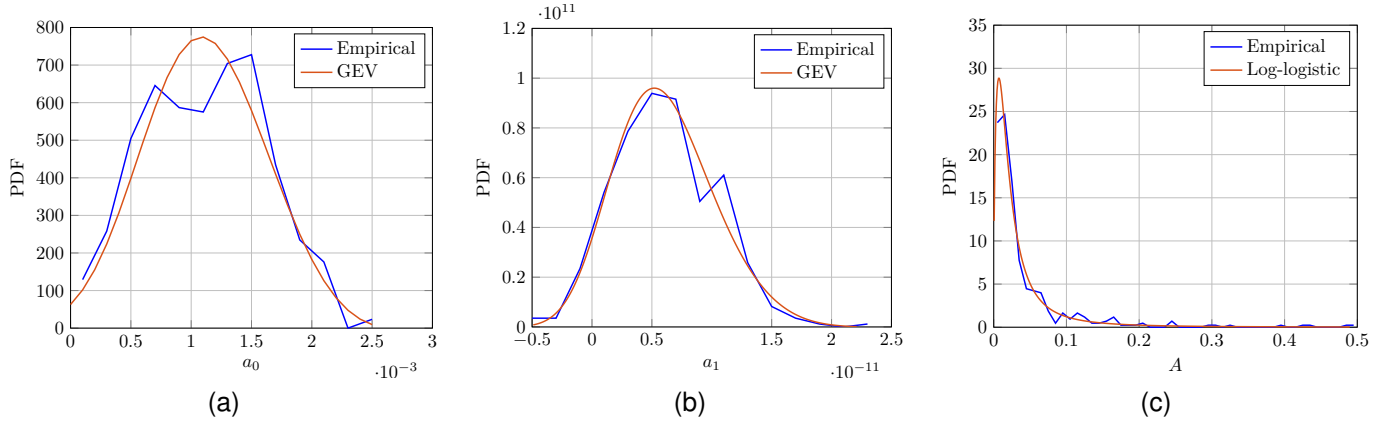


Figure 3. Empirical and fitted PDFs of the attenuation coefficients a_0 and a_1 and the normalization coefficient A .

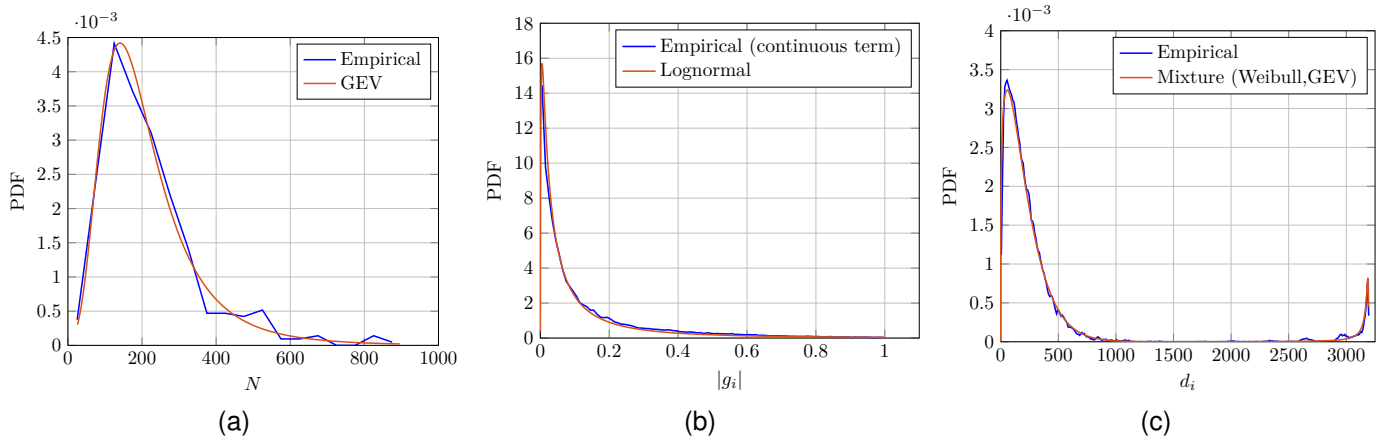


Figure 4. Empirical and fitted PDFs of the number of dominant paths, N , the modulus of the path gains $|g_i|$ and the path lengths d_i .

some parameters, more elaborate models consisting of mixture distributions have been considered.

The mean and standard deviation of the MPM parameters are given in Table III. The fitting statistical distributions with their corresponding parameter values are summarized in Table IV. These reported results allow future replicability of this study and simplify the development of improved statistical models.

The empirical PDFs (EPDFs) of the MPM parameters are reported in Fig. 3 and Fig. 4. Regarding a_0 and a_1 , whose EPDFs are shown in Fig. 3 (a) and (b), respectively, the distribution that gives the best fit is the GEV (p -value= 0.286 for a_0 and 0.8941 for a_1), although the normal distribution also gives a high p -value (0.1967 for a_0 and 0.5664 for a_1). In practice, the GEV is a family of three types of extreme value

distributions, namely type I, or Gumbel (or log-Weibull) [33], type II, or Fréchet, and type III, or Weibull distribution. This result makes sense since the GEV is the limit distribution of properly normalized maxima of a sequence of independent and identically distributed random variables. The GEV distribution for a_0 is justified since it represents the maximum (or the minimum in case of negative values of a_1) of the channel attenuation profile for the identified trend of each measured CFR.

Regarding the normalization coefficient, A , whose EPDF is displayed in Fig. 3 (c), the Log-logistic gives the largest p -value (0.909) although, although the GEV and the log-normal also give high values (p -values 0.788 and 0.4536, respectively). The latter is not surprising, as A is determined as the maximum value of the path gains, $|g_i|$, of each fitted

Table II
PARAMETERS OF THE FITTING EXPRESSIONS DISPLAYED IN FIG. 2.

Fitting expression	α	β	γ
$\hat{a}_0 = \alpha + \beta \cdot G$ (dB)	$-1.8669 \cdot 10^{-4}$	$-3.4066 \cdot 10^{-5}$	-
$\hat{N} = \alpha + \beta \cdot ds$ (μ s) + $\gamma \cdot G$ (dB)	40.4009	185.7535	4.5097
$\hat{A} = \alpha \cdot e^{\beta \cdot G}$ (dB)	$8.2517 \cdot 10^{-1}$	$1.0636 \cdot 10^{-1}$	-

Table III
MEAN AND STANDARD DEVIATION OF THE MPM PARAMETERS

MPM parameter	mean	standard deviation
Atten. coeff. (a_0)	0.0011	5.0089e-4
Atten. coeff. (a_1)	6.0953e-12	4.1137e-12
Norm. coeff. (A)	0.0422	0.0649
Number of dominant paths (N)	217.8427	1.3457
Path gains ($ g_i $)	0.1384	0.1859
Path lengths (d_i)	343.9491	633.4392

channel.

Regarding the probability distribution of the number of dominant paths, N , while this magnitude can only take non-negative integer values, discrete distributions like the binomial and Poisson ones give very poor fitting to the actual set of values. Hence, N has been considered as a discretized version of a continuous random variable. This same approach has been also applied to fit the path length, d_i . By doing so, the GEV gives the best fit (p -value= 0.86752) to the number of dominant paths, N , whose EPDF is displayed in Fig. 4 (a). As a matter of fact, N represents the maximum number of dominant paths that actively contribute to reconstruct each measured CFR.

Concerning the characterization of the path gain, its absolute value, $|g_i|$, is considered for the sake of simplicity, as the EPDF of g_i shows a symmetric behavior around the y -axis. The statistical characterization of $|g_i|$ must take into account that the normalization process used to force $g_i \in [-1, 1]$ in each fitted channel causes the probability of $|g_i| = 1$ to be non-zero. Hence, $|g_i|$ has to be modeled by a mixed random variable (RV) consisting of a continuous component and a discrete term at $|g_i| = 1$. Fig. 4 (b) shows that the continuous term of the EPDF can be fitted by a log-normal RV. Accordingly, the overall PDF can be expressed as $f(|g_i|) = \pi_0 q(|g_i| | \mu, \sigma) + \pi_1 \delta(|g_i| - 1)$, where $q(\cdot | \mu, \sigma)$ denotes the PDF of a log-normal RV with parameters μ and σ and $\delta(\cdot)$ is the Dirac delta function. The value of these parameters are given in Table IV.

The EPDF of d_i , displayed in Fig. 4 (c), exhibits a bimodal behavior, with maxima around $d_i = 50$ m and $d_i = 3195$ m. The latter is an effect of the use of the discrete frequency domain version of (1), which obliges to set a limit for the largest path length. Since the observed bimodal behavior cannot be obtained with any of the distributions indicated above, we have resorted to mixture models. It has been found that the Weibull distribution gives a good fitting to the values of $d_i \leq 1500$ while the GEV, shifted and reflected about $d_{N-1} = \frac{N-1}{N}L$, adequately fits the values of $d_i > 1500$. Hence, the PDF of d_i can be modeled as $f(d_i) = \pi_0 g_0(d_i | \lambda_0, k_0) + \pi_1 g_1(d_{N-1} - d_i | k_1, \sigma_1, \mu_1)$, where $g_0(\cdot | \lambda_0, k_0)$ denotes the PDF of a Weibull distribution with scale and shape parameters λ_0 and k_0 , respectively, and $g_1(\cdot | k_1, \sigma_1, \mu_1)$ is the PDF of a GEV distribution with location, scale and shape parameters k_1 , σ_1 and μ_1 , respectively, whose values are given in Table IV. As shown in Fig. 4 (c), the PDF of the proposed mixture gives a

good fitting to the empirical one.

Table IV
FITTING DISTRIBUTIONS OF THE MPM PARAMETERS

MPM parameter	Distribution	Distribution parameters
Atten. coeff. a_0	GEV	$k = -0.2744$ $\sigma = 4.9492 \cdot 10^{-4}$ $\mu = 9.3370 \cdot 10^{-4}$
Atten. coeff. a_1	GEV	$k = -0.1781$ $\sigma = 3.8980 \cdot 10^{-12}$ $\mu = 4.4536 \cdot 10^{-12}$
Norm. coeff. A	Log-logistic	$\mu = -3.8584$ $\sigma = 0.6710$
Number of dominant paths N	GEV	$k = 0.1641$ $\sigma = 84.3237$ $\mu = 153.5548$
Path gains $ g_i $	Mixture (lognormal, $ g_i = 1$)	$\pi_0 = 1 - \pi_1$ $\pi_1 = 4.6017 \cdot 10^{-3}$ $\mu = -2.9139$ $\sigma = 1.5445$
Path lengths d_i	Mixture (Weibull, GEV)	$\pi_0 = 9.5074 \cdot 10^{-1}$ $\pi_1 = 1 - \pi_0$ $\lambda_0 = 2.1894 \cdot 10^2$ $k_0 = 1.2314$ $k_1 = 1.3432$ $\sigma_1 = 42.5933$ $\mu_1 = 27.4299$

In order to get an in-depth analysis of the behavior of d_i , Fig. 5 (a) displays the path length, d_i , vs the dominant path index, i , for some illustrative measured channels. For the sake of clarity, the markers corresponding the same channel have been linked by a dashed line of the the same color. As seen, all channels have a set of paths whose length is uniformly distributed from zero (or almost zero) and a given value that depends on the channel. However, some channels, like Ch. 3-7, also have a set of paths with very large length. In many cases, like Ch. 3 and Ch. 4, there are no paths with intermediate distances. This behavior is related to the frequency selectivity of the channel: the larger the frequency selectivity, the large the distances of the paths required to synthesize it. This can be observed in Fig. 5 (b), where the scatter plot of the median value of the dominant path lengths vs the delay spread of each measured channel is given. As observed, channels with higher delay spread values (larger frequency selectivity) need larger paths to be synthesized. Furthermore, it is also expected that the higher the number of dominant paths, the larger the median length of the paths. Fig. 5 (c) confirms this end by showing a strong linear relationship between them.

C. Comparison with Other Works

The MPM parameter distributions that have been just presented are herein compared with those heuristically or empirically obtained in previous scientific works. For example the presented statistical analysis confirms the assumptions made in [21], which statistically extended the MPM in (1) relying on the initial idea presented in [10]. Hence, it was inferred in [21] that the path gains g_i turn out to be log-normally distributed

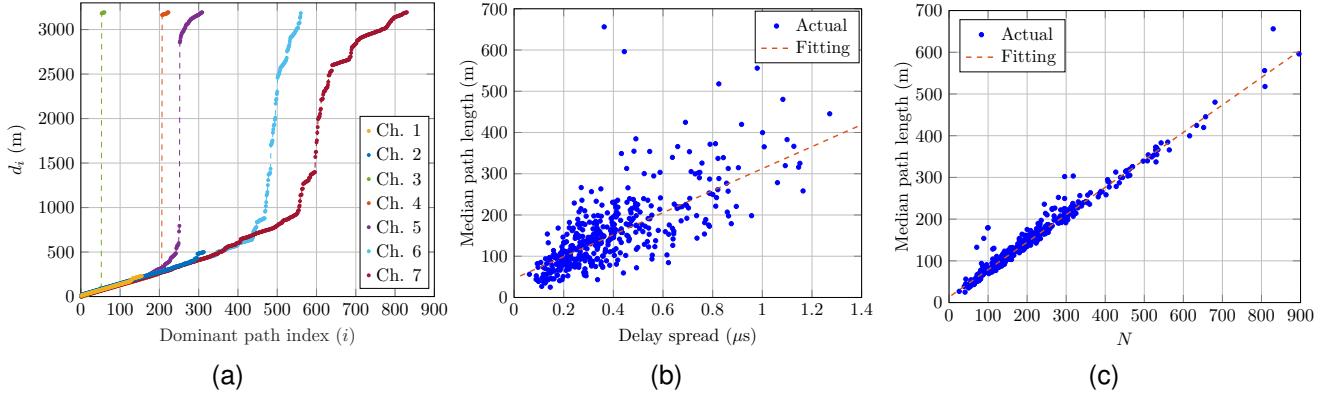


Figure 5. (a) Dominant path length vs dominant path index for some illustrative measured channels; (b) scatter plot of the median value of the dominant path length vs the delay spread for the set of measured channels; (c) scatter plot of the median value of the dominant path length vs the number of dominant paths for the set of measured channels.

variables multiplied by a random flip sign. The main difference is found for the statistics of N , supposed to have a Poisson distribution in [21], but that results into a GEV one. This difference was already hypothesized in [21] and is also justified by the different considered databases. The path lengths, d_i , were assumed to be log-normally distributed in [21], while the mixture of a Weibull and GEV has been obtained in this work. Additionally, the characterization method proposed in this paper provides a statistics for the other parameters, i.e., a_0 , a_1 , and A .

Other results concerning the MPM parameters distribution are listed in [34](Tab. 1), that extends the model in (1) to the MIMO transmission. In this case, the path gains g_i are assumed uniformly distributed in $[-1, 1]$ and the attenuation coefficient a_1 turns out to be constant. While, K is normally distributed and a_0 exhibits a shifted exponential distribution. Instead, the channel median A is uniformly or exponentially distributed depending on the considered channels. The same results are also summarized in [35, Tab. 2.10].

D. Relationship Between Parameters

The development of MPM-based models requires a complete characterization of the involved parameters. This includes both their marginal PDFs, which have given in the previous subsection, and their joint distribution, which are examined in this one.

First, the relation between the path length, d_i , and the number of dominant paths, N , is explored. To this end, the probability distribution of the path length conditioned on N , $P_r(d_i|N)$ is estimated. Obtained results are given in Fig. 6, which gives additional details on the already observed bimodal behavior of the EPDF of d_i . As seen, there are almost no paths with lengths in the range from 1000 – 3000 m, approximately, except for the case where N is very large, in which some paths with lengths in this range can be found. The values of d_i are concentrated in the low length region and in the region around 3000 m, being (approximately) uniformly distributed from zero (or almost zero) in the low length region. Furthermore, the range of path lengths in the low region increases with the number of dominant paths.

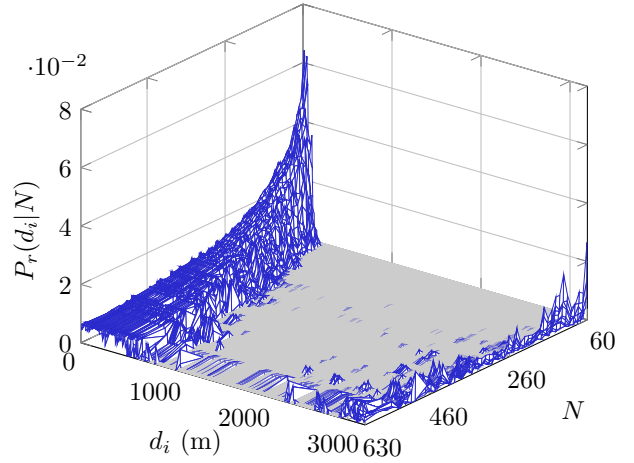


Figure 6. Conditional probability of the path length, d_i , given the number of dominant paths, N , estimated over the set of measured channels.

Next, the relation between the absolute value of the path gain and the path length is assessed by estimating the conditional PDF of $|g_i|$ given d_i , $f_{|g_i|}(|g_i||d_i)$. Results are displayed in Fig. 7. Interestingly, $|g_i|$ tends to a uniform distribution in the interval $(0, 1)$ for very low values of d_i . As the path length increases, the range of values of $|g_i|$ decreases until it tends, again, to a uniform one in the interval $(0, 1)$ for path lengths around 3000 m. There is a clearly noticeable gap for path lengths between 1000 – 2500 (approximately), where the few existing paths have very low gains.

Finally, the correlation between the path gains is explored. Since the decimation process described in Section III.III-A yields a different number of paths for each measured channel, the following procedure is employed to allow comparing results from different channels. In order to distinguish the MPM model parameters before the decimation process is applied from the ones resulting after it, let us denote the latter by using tilded symbols. Hence, the original set of path lengths and path gains are expressed as d_n and g_n , respectively, with $0 \leq n \leq N - 1$, where $N = 2554$, and their corresponding sets after the decimation process as \tilde{d}_i and \tilde{g}_i , respectively, with

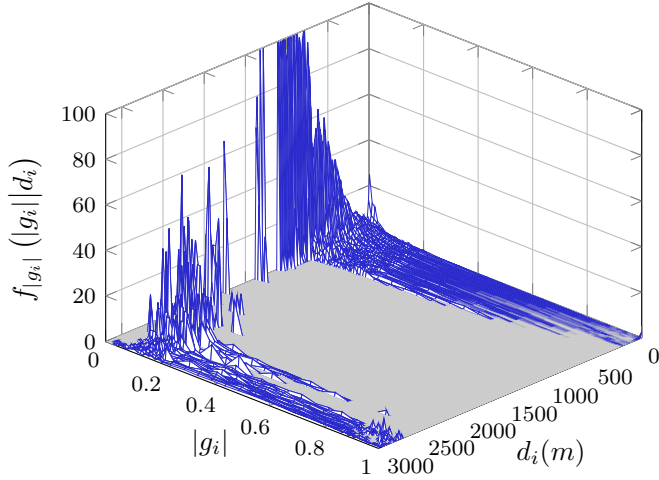


Figure 7. Conditional PDF of $|g_i|$ given the path length, d_i , estimated over the set of measured channels.

$0 \leq i \leq \tilde{N}$, where \tilde{N} is the number of dominant paths after the decimation process. These magnitudes are related as

$$g_n = \begin{cases} \tilde{g}_i & \text{if } \exists i \mid \tilde{d}_i = d_n \\ 0 & \text{otherwise} \end{cases}. \quad (16)$$

In order to explore the correlation among the path gains, the deterministic autocorrelation function (ACF) of $|g_n|$ for each measured channel, $R_{|g_n|}(n) = \frac{1}{N} \sum_{m=0}^{N-n-1} |g_{n+m}| |g_m|$, for $0 \leq n \leq N$, is computed and normalized. Fig. 8 depicts its average value (over the set of measured channels) and the envelope of the ACF of all channels. As seen, the ACF decreases very rapidly, with values below 0.5 for $n \geq 8$ and below 0.3 for $n \geq 40$, and slightly regrows for large values of n due to the behavior already shown in Fig. 7.

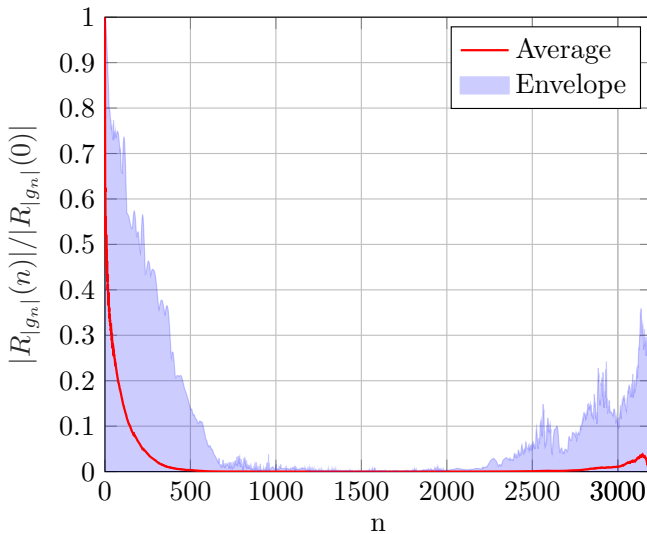


Figure 8. Average and envelope of the normalized deterministic ACF of $|g_n|$ computed over the set measured channels.

V. CONCLUSION

The MPM is one of the most common top-down models adopted in the literature about PLC. This paper explores the

parameterization of this model, which was originally proposed for low-voltage power distribution networks in the band up to 20 MHz, for the indoor broadband scenario in the band up to 80 MHz. Since the number of parameters that result from the extension of the MPM model to this context is extremely large, some of them have been imposed on the basis of common sense intuition, others, such as the attenuation parameters and the set of initial path lengths, have been chosen according to physical assumptions, and the remaining ones are analytically retrieved by means of a WLS fitting.

Since the number of parameters that result after the WLS fitting is still excessively large, only the dominant paths that actively contribute to synthesize the CFR have been selected according to a proposed decimation procedure that yields a more compact model. The implemented selection method determines the number of significant paths subject to a constraint on the maximum value of the NRMSE.

Once the MPM parameters have been computed according to the proposed strategy, they are related to the characteristics of the actual CFRs like the frequency selectivity and the average channel gain. Suitable distributions that fit the empirical PDF of each parameter are also given. Finally, the relation between the most relevant parameters of the model is explored. Provided results will aid the development improved channels models for indoor broadband PLC.

REFERENCES

- [1] L. Yonge, J. Abad, K. Afkhamie, L. Guerrieri, S. Katar, H. Lioe, P. Pagani, R. Riva, D. M. Schneider, and A. Schwager, "An Overview of the HomePlug AV2 Technology," *Journal of Electrical and Computer Engineering*, vol. 2013, pp. 1–20, 2013.
- [2] "Unified high-speed wireline-based home networking transceivers - System architecture and physical layer specification," ITU-T Recommendation G.9960, International Telecommunications Union, July 2015.
- [3] IEEE Std 1901-2020, "IEEE Standard for Broadband over Power Line Networks: Medium Access Control and Physical Layer Specifications."
- [4] S. Bush, S. Goel, and S. Simard, "IEEE vision for smart gridcommunications: 2030 and beyond roadmap," IEEE Standards Association, 2013, pp. 1-19.
- [5] G. Prasad and L. Lampe, "Full-duplex power line communications: Design and applications from multimedia to smart grid," *IEEE Communications Magazine*, vol. 58, no. 2, pp. 106–112, Feb. 2020.
- [6] D. Righini and A. M. Tonello, "MIMO in-band-full-duplex PLC: Design, analysis and first hardware realization of the analog self-interference cancellation stage," *IEEE Open Journal of the Communications Society*, vol. 2, pp. 1344–1357, 2021.
- [7] F. J. Cañete, G. Prasad, and L. Lampe, "In-band full-duplex MIMO PLC systems for relaying networks," *Digital Communications and Networks*, 2023.
- [8] J. A. Cortés, F. J. Cañete, and L. Díez, "Channel estimation for OFDM-based indoor broadband power line communication systems," *Journal of Communications and Networks*, vol. 25, no. 2, pp. 151–166, Apr. 2023.
- [9] M. Zimmermann and K. Dostert, "A multipath model for the powerline channel," *IEEE Transactions on Communications*, vol. 50, no. 4, pp. 553–559, April 2002.
- [10] A. M. Tonello, "Wideband impulse modulation and receiver algorithms for multiuser power line communications," *EURASIP Journal on Advances in Signal Processing*, pp. 1–14, 2007.
- [11] F. J. Cañete, J. A. Cortés, L. Díez, and J. T. Entrambasaguas, "A channel model proposal for indoor power line communications," *IEEE Communications Magazine*, vol. 49, no. 12, pp. 166–174, December 2011.
- [12] I. Povedano, F. Crespo, J. A. Cortés, F. J. Cañete, and L. Díez, "A statistical model for indoor SISO PLC channels," in *IEEE International Symposium on Power Line Communications and its Applications (IS-PLC)*, 2023.

- [13] F. J. Cañete, L. Díez, J. A. Cortés, and J. T. Entrambasaguas, "Broadband modelling of indoor power-line channels," *IEEE Transactions on Consumer Electronics*, pp. 175–183, Feb 2002.
- [14] S. Galli and T. C. Banwell, "A deterministic frequency-domain model for the indoor power line transfer function," *IEEE Journal on Selected Areas on Communications*, vol. 24, no. 7, pp. 1304–1316, July 2006.
- [15] H. Philipps, "Modelling of power line communication channels," in *Proceedings of the International Symposium on Power Line Communications and its Applications (ISPLC)*, 1999, pp. 14–21.
- [16] —, "Development of a statistical model for powerline communication channels," in *International Symposium on Power Line Communications and its Applications (ISPLC)*, 2000.
- [17] T. Esmailian, F. R. Kschischang, and P. G. Gulak, "In-building power lines as high-speed communication channels: channel characterization and a test channel ensemble," *International Journal of Communications*, vol. 16, pp. 381–400, June 2003.
- [18] A. M. Tonello and F. Versolatto, "Bottom-up statistical PLC channel modeling - Part I: Random topology model and efficient transfer function computation," *IEEE Transactions on Power Delivery*, vol. 26, no. 2, pp. 891–898, 2011.
- [19] F. Versolatto and A. M. Tonello, "An MTL theory approach for the simulation of MIMO power line communication channels," *IEEE Transactions on Power Delivery*, vol. 26, no. 3, pp. 1710–1717, 2011.
- [20] J. A. Corchado, J. A. Cortés, F. J. Cañete, and L. Díez, "An MTL-Based Channel Model for Indoor Broadband MIMO Power Line Communications," *IEEE Journal on Selected Areas in Communications*, vol. 34, no. 7, pp. 2045–2055, July 2016.
- [21] A. M. Tonello, F. Versolatto, B. Bejar, and S. Zazo, "A fitting algorithm for random modeling the PLC channel," *IEEE Transactions on Power Delivery*, vol. 27, no. 3, pp. 1477–1484, 2012.
- [22] A. Canova, N. Benvenuto, and P. Bisaglia, "Receivers for MIMO-PLC channels: Throughput comparison," in *IEEE International Symposium on Power Line Communications and its Applications (ISPLC)*, 2010, pp. 114–119.
- [23] P. Pagani and A. Schwager, "A statistical model of the in-home MIMO PLC channel based on European field measurements," *IEEE Journal on Selected Areas in Communications*, vol. 34, no. 7, pp. 2033–2044, Jul. 2016.
- [24] F. J. Cañete, J. A. Cortés, L. Díez, and J. T. Entrambasaguas, "Analysis of the cyclic short-term variation of indoor power line channels," *IEEE Journal on Selected Areas on Communications*, vol. 24, no. 7, pp. 1327–1338, July 2006.
- [25] M. Babic, M. Hagenau, K. Dostert, and J. Bausch, "D4: Theoretical postulation of PLC channel model," Opera, Tech. Rep., 2005.
- [26] Y.-R. Chien, "Iterative channel estimation and impulsive noise mitigation algorithm for OFDM-based receivers with application to power-line communications," *IEEE Transactions on Power Delivery*, vol. 30, no. 6, pp. 2435–2442, Dec. 2015.
- [27] J. Huang, Q. Wan, and P. Wang, "Robust approach for channel estimation in power line communication," *Journal of Communications and Networks*, vol. 14, no. 3, pp. 237–242, 2012.
- [28] M. Gay, L. Lampe, and A. Lampe, "SVD-based de-noising and parametric channel estimation for power line communication systems," in *IEEE International Symposium on Power Line Communications and its Applications (ISPLC)*, 2016.
- [29] A. Tonello and F. Pecile, "A filtered multitone (FMT) modulation modem with an efficient digital implementation for multiuser powerline communications," in *Proceedings of the IEEE International Symposium on Power Line Communications and its Applications (ISPLC)*, March 2007.
- [30] A. M. Tonello, F. Versolatto, and A. Pittolo, "In-home power line communication channel: statistical characterization," *IEEE Transactions on Communications*, vol. 62, no. 2, pp. 2096–2106, 2014.
- [31] A. F. Molish, *Wireless Communications*, 2nd ed. John Wiley & Sons Ltd., 2011.
- [32] P. J. Bickel and K. A. Doksum, *Mathematical Statistics. Basic Ideas and Selected Topics*. Chapman and Hall/CRC, 2015, [On-line] <https://www.taylorfrancis.com/books/9781498740418>.
- [33] E. J. Gumbel, "Statistical theory of extreme values and some practical applications. A series of lectures," U.S. National Technical Reports Library. Applied mathematics series, 1954, [On-line] <https://books.google.it/books?id=SNpJAAAAMAAJ>.
- [34] R. Hashmat, P. Pagani, A. Zeddani, and T. Chonave, "A channel model for multiple-input multiple output in-home power line networks," in *IEEE International Symposium on Power Line Communications and Its Applications (ISPLC)*, 2011, pp. 35–41.
- [35] L. Lampe, A. M. Tonello, and T. G. Swart, Eds., *Power line communications: principles, standards and applications from multimedia to Smart Grid*, 2nd ed. Wiley, June 2016.